Non-Newtonian Granular Fluids: Simulation and Theory

M. Alam
Engineering Mechanics Unit, Jawaharlal Nehru Center for Advanced Scientific Research
Jakkur P.O., Bangalore 560064, India

S. Luding
Particle Technology, DelftChemTech, TU Delft, Julianalaan 136, 2628 BL Delft, The Netherlands

ABSTRACT: Rheological properties of granular fluids are probed via event-driven simulations of the inelastic hard-sphere model. We find that granular fluids support large *normal stress differences* for the whole range of densities, clearly indicating their non-Newtonian rheology. Interestingly, both *first* ($\mathcal{N}_1$) and *second* ($\mathcal{N}_2$) normal stress differences undergo *sign-reversals* with density. While $\mathcal{N}_1$ changes its sign in the *dense* limit, $\mathcal{N}_2$ changes its sign in the *dilute* limit. The *origin* of such *sign-reversals* is tied to the *microstructural* reorganization of particles and to anisotropy in general. We briefly outline a viscoelastic constitutive model for granular fluids which allows the *sign-reversals* of both first and second normal stress differences.

1 INTRODUCTION

Granular materials behave like a fluid under strong external driving. Unlike normal fluids, however, granular fluids possess prominent *non-Newtonian* properties, like the normal stress differences. For a simple fluid (e.g. air and water), such normal stress differences are of *infinitesimal* magnitudes, but they can be of the order of its isotropic pressure in a dilute granular gas (Jenkins & Richman 1988; Sela & Goldhirsch 1998; Alam & Luding 2003, 2003a). Since the normal stresses are known to be responsible for many interesting flow-features (e.g. rod-climbing, secondary flows, etc.) in non-Newtonian fluids (Bird et al. 1979), it is of interest to understand the non-Newtonian characteristics of granular fluids.

Moreover, prior knowledge of rheology is needed to make meaningful progress in developing constitutive models. The major objective of the present work is to understand the non-Newtonian rheology and the microstructural features of a granular fluid. Another objective is to test and validate the available constitutive models against the rheological data obtained from simulations.

We simulate the uniform shear flow configuration using the standard smooth inelastic hard-sphere model. The details of the simulation technique and the relevant macroscopic quantities are described in section 2. The simulation results on the normal stress differences in both 2D and 3D are discussed and compared with relevant theory in section 3. Possible modelling approaches to incorporate the normal stress differences are briefly discussed in section 4. Conclusions are provided in section 5.

2 HARD SPHERES: UNIFORM SHEAR FLOW

We use the inelastic hard-sphere model for which the collisions are instantaneous and the simulation moves in time from one collision to the next and so on. The pre- and post-collisional velocities of two colliding particles are related by the expression:

$$\mathbf{k}\cdot\tilde{\mathbf{c}}'_{ji} = -e(\mathbf{k}\cdot\tilde{\mathbf{c}}_{ji}), \tag{1}$$

where $\tilde{\mathbf{c}}_{ji} = \tilde{\mathbf{c}}_j - \tilde{\mathbf{c}}_i$ is the pre-collisional velocity of particle j relative to i ($\tilde{\mathbf{c}}'_{ji}$ being the corresponding post-collisional relative velocity), $\mathbf{k}_{ji} = \mathbf{k}$ the unit vector directed from the center of the particle j to that of particle i, and e is the coefficient of normal restitution, with $0 \leq e \leq 1$. We drive a collection of smooth inelastic hard-spheres in a cubic box of size $\tilde{L}$ by the uniform shear flow, using the Lees-Edwards boundary condition (Allen & Tildesley 1989). Let $\tilde{x}$ and $\tilde{y}$ ($\tilde{z}$) be the streamwise and transverse directions, respectively, with the origin of the coordinate-frame being positioned at the centre of the box. In the following we restrict to a monodisperse system of particles of diameter, $\tilde{d}$, and material density $\tilde{\rho}$.

The macroscopic stress and the related transport coefficients (pressure, shear viscosity, and the normal stress differences) are calculated from the simulation data. Defining $\tilde{L}$, $\tilde{\gamma}^{-1}$ and $\tilde{\gamma}\tilde{L}$ as the reference scales for length, time and velocity, respectively, the relevant

dimensionless variables are:

$$d = \frac{\tilde{d}}{\tilde{L}}, \quad (\mathbf{c}, \mathbf{u}, \mathbf{C}) = \frac{1}{\tilde{\gamma}\tilde{L}}(\tilde{\mathbf{c}}, \tilde{\mathbf{u}}, \tilde{\mathbf{C}}), \tag{2}$$

where $\tilde{\mathbf{u}}$ is the mass-averaged velocity, $\tilde{\mathbf{C}} = \tilde{\mathbf{c}} - \tilde{\mathbf{u}}$ the peculiar velocity of particles. The total stress and the granular energy are rescaled by the average momemtum flux density and kinetic energy, respectively:

$$\mathbf{P} = \frac{\tilde{\mathbf{P}}}{\tilde{\rho}\tilde{d}^2\tilde{\gamma}^2}, \quad T = \frac{\tilde{T}}{\tilde{d}^2\tilde{\gamma}^2}. \tag{3}$$

The nondimensional total stress is calculated from

$$\begin{aligned} \mathbf{P} &= \mathbf{P}^k + \mathbf{P}^c \\ &= \frac{\pi}{6}\left[\sum_{i=1}^{N} \mathbf{C}_i \otimes \mathbf{C}_i + \frac{d}{\tau_d}\sum_{collisions}(\mathbf{I}_{ij} \otimes \mathbf{k})\right], \end{aligned} \tag{4}$$

where $\mathbf{P}^k$ and $\mathbf{P}^c$ are the kinetic and collisional contributions to the total stress $\mathbf{P}$, respectively, and $\mathbf{I}_{ij}$ is the collisional impulse. For the collisional stress, the sum is taken over all collisions during the averaging time window τ_d. Note that the trace of the kinetic part of the stress tensor is used to calculate the granular energy.

Now we decompose the total stress, defined in the *compressive* sense, in the following way:

$$\mathbf{P} = \mathbf{P}^k + \mathbf{P}^c = p\mathbf{1} + \Pi, \tag{5}$$

where p is the pressure, Π the pressure deviator and $\mathbf{1}$ the unit tensor. (Note that the off-diagonal components of the pressure deviator, Π_{xy}, is related to the *shear viscosity*, see Alam & Luding 2003, 2003a.) The diagonal components of the pressure deviator could be different from zero, giving rise to *normal stress differences*:

$$\mathcal{N}_1 = \frac{(\Pi_{xx} - \Pi_{yy})}{p}, \tag{6}$$

$$\mathcal{N}_2 = \frac{(\Pi_{yy} - \Pi_{zz})}{p}. \tag{7}$$

The former is called the *first* normal stress difference, and the latter the *second* normal stress difference. Note that we have scaled these quantities by pressure to discern their relative magnitudes with respect to pressure. For a Newtonian fluid, $\mathcal{N}_1 = 0$ and $\mathcal{N}_2 = 0$. Hence non-zero values of $\mathcal{N}_1$ and $\mathcal{N}_2$ are indicators of the *non-Newtonian* character of the fluid.

The spheres are initially placed randomly in the cubic box, and the initial velocity field is composed of the uniform shear and a small Gaussian random part. An event-driven algorithm (Allen & Tildesley 1989) is then used to simulate instantaneous binary collisions. At the steady state, the uniform shear flow attains a constant granular energy due to the balance between the shear work and the collisional dissipation, After reaching this steady-state, the simulation was allowed to run for at least another 5000 collisions per particle to gather data to calculate the rheological and microstructural quantities. The total number of particles was fixed at $N = 1000$.

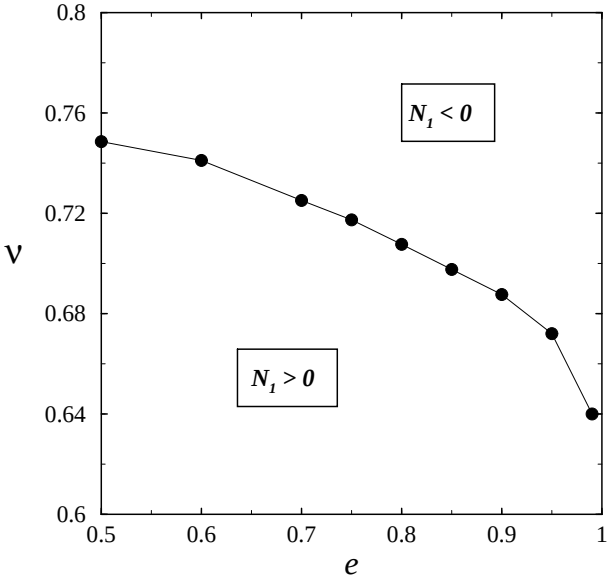

Figure 1. Phase diagram delineating the regions of positive and negative $\mathcal{N}_1$ in the (ν, e)-plane in 2D.

3 RESULTS AND DISCUSSION

3.1 *Two dimensions (2D)*

Before presenting results for 3D, we briefly recall our earlier results (Alam & Luding 2003a) for the first normal stress difference, $\mathcal{N}_1$, in two-dimensions (2D). It was found that the granular fluid is non-Newtonian with a measurable $\mathcal{N}_1$ which is *positive* (if the stress is defined in the *compressive* sense as in the present work) in the dilute limit. Interestingly, however, $\mathcal{N}_1$ *changes* from positive to negative at a critical density in the dense regime. By decomposing $\mathcal{N}_1$ into the kinetic and collisional contributions, $\mathcal{N}_1 = \mathcal{N}_1^k + \mathcal{N}_1^c$, we found that while $\mathcal{N}_1^k$ is always positive and decays to zero in the dense limit, $\mathcal{N}_1^c$ has a *non-monotonic* variation with density. In particular, $\mathcal{N}_1^c$ increases from zero in the dilute limit as ν increases, reaches a maximum at some value of ν and then decreases, eventually becoming *negative* in the dense limit. The density at which $\mathcal{N}_1^c = 0$ ($\nu \equiv \nu_1$) depends crucially on the level of micro-scale dissipation; in particular, ν_1 increases as the coefficient of restitution decreases. This is evident from Fig. 1 where we have displayed the phase-diagram in the (ν, e)-plane by identifying the regions where $\mathcal{N}_1$ is positive/negative.

The behaviour of the first normal stress difference in the dense limit is tied to shear-induced collisional anisotropies (Alam & Luding 2003a). In particular, the topology of the collision-angle distribution $C(\theta)$,

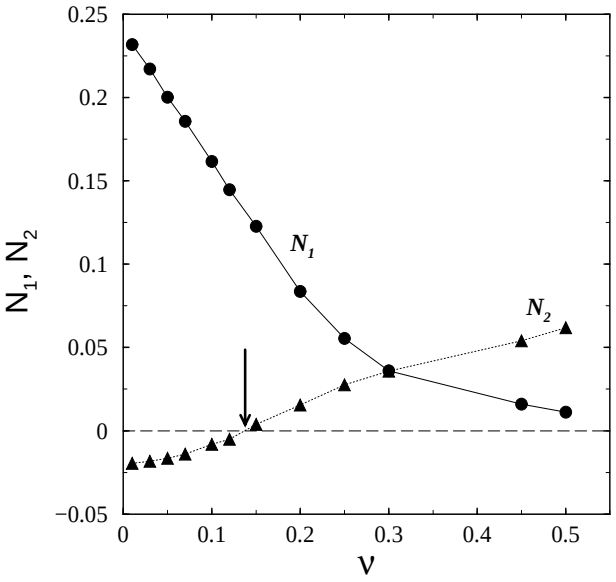

Figure 2. Variations of $\mathcal{N}_1$ and $\mathcal{N}_2$ with solid fraction, for restitution coefficient $e = 0.9$. The arrow indicates critical solid fraction at which $\mathcal{N}_2$ changes sign.

where θ is the polar angle, changes drastically, with collisions occurring at certain preferred angles on the upstream-faces of the colliding pairs. The *origin* of the *sign-reversal* of $\mathcal{N}_1$ is, thus, correlated with a preferred value of the average collision angle, $\theta_{av} = \pi/4 \pm \pi/2$, averaged over the *upstream*-faces of the colliding particles.

3.2 *Three dimensions (3D)*

Figure 2 shows the variations of two normal stress differences ($\mathcal{N}_1$ and $\mathcal{N}_2$) with the solid fraction; the restitution coefficient is $e = 0.9$. The first normal stress difference $\mathcal{N}_1$ is positive and maximal in the Boltzmann limit ($\nu \to 0$) and decreases in magnitude with increasing density. For the parameters used here, $\mathcal{N}_1$ did not undergo a *sign-reversal* even at $\nu = 0.52$. But increasing the value of the restitution coefficicient to $e = 0.99$, we found that the *sign-reversal* occurred at a critical density $\nu_1 \approx 0.52$. This obsevation mirrors our results in 2D (Alam & Luding 2003a), except that the value of the critical density ν_1 is lower than that in 2D (as expected). The microstructural origin of the sign-reversal of $\mathcal{N}_1$ is again tied to the anisotropic structure of the collision-angle distribution as in 2D.

We observe in Fig. 2 that the second normal stress difference $\mathcal{N}_2$ is negative in the Boltzmann limit ($\nu \to 0$), increases with increasing density, becomes *positive* at a critical density $\nu_2 \approx 0.135$, and increases monotonically thereafter. The second normal stress difference is of the order of about seven per-cent of the total stress at the highest densities examined here. Note that the sign-reversal $\mathcal{N}_2$ is also apparent in the work of Campbell (1989).

At very low densities, the collisional components of the stress tensor are much smaller than their kinetic counterpart. At moderate densities, the collisional contribution becomes more important and at higher densities it is dominant. The increase of $\mathcal{N}_2$ with density thus links it to the collisional contributions to stress. Preliminary results indicate that the distribution of the mean free paths (along three directions) changes with increasing density. This is connected to the collision angle, as in 2D, and is responsible for the *sign-reversal* of $\mathcal{N}_2$. A detailed investigation of this issue will be taken up soon.

Finally, we compare our results with the work of Sela & Goldhirsch (1998) who derived constitutive expressions for the stress tensor upto the Burnett-order for a dilute granular fluid ($\nu \to 0$). For uniform shear flow, it can be verified that the expressions for normal stress differences take the following forms:

$$\mathcal{N}_1 = \frac{(1.6735\epsilon - 0.04315\epsilon^2)}{(1.2996 + 0.0966\epsilon)} \quad (8)$$

$$\mathcal{N}_2 = -\frac{(0.14189\epsilon - 0.003659\epsilon^2)}{(1.2996 + 0.0966\epsilon)} \quad (9)$$

where $\epsilon = (1 - e^2)$ is the degree of inelasticity. Clearly, for a given inelasticity $\epsilon \neq 0$, $\mathcal{N}_1 > 0$ and $\mathcal{N}_2 < 0$ in the Boltzmann limit. For example, the values of normal stress differences are $\mathcal{N}_1 \approx 0.24$ and $\mathcal{N}_2 \approx -0.0203$ for $e = 0.9$; the corresponding results from our simulation are $\mathcal{N}_1 \approx 0.232$ and $\mathcal{N}_2 \approx -0.0196$ at a solid fraction of $\nu = 0.01$. We should mention here that the perfect elastic limit ($e \to 1$) is non-trivial, and the normal stresses in the elastic limit remain *non-zero* (but of infinitesimal magnitude). The effect of inelasticity is merely to amplify the magnitudes of both $\mathcal{N}_1$ and $\mathcal{N}_2$, making the normal stresses of order $O(\epsilon)$ for granular fluids.

4 RELAXATION TYPE MODELS

Here we attempt to describe the normal-stress behaviour of a granular fluid using relaxation-type constitutive models. Prior literature on the dense-gas kinetic theory indicates that such a stress relaxation mechanism does also exist in granular fluids (Jenkins & Richman 1988; Sela & Goldhirsch 1998). Moreover, the recent work of Zhang & Rauenzahn (1997) suggests that such viscoelastic stress relaxation mechanism exists even in dense granular flows.

Let us first consider the viscoelastic relaxation model of Jin & Slemrod (2001) who have regularized the Burnett order equations of Sela & Goldhirsch (1998) for a low-density granular fluid. Their proposed equation for the pressure deviator can be written as

$$\Pi + \tau_1 \left(\frac{D\Pi}{Dt} - \mathbf{L}^T \cdot \Pi - \Pi \cdot \mathbf{L} + \tfrac{2}{3} tr(\Pi \cdot \mathbf{L}) \mathbf{1} \right) + \tau_2 \left(\mathbf{S} \cdot \Pi + \Pi \cdot \mathbf{S} - \tfrac{2}{3} tr(\Pi \cdot \mathbf{S}) \mathbf{1} \right) = \Pi^{eq}, \quad (10)$$

where

$$\Pi^{eq} = -2\mu \mathbf{S} - (\zeta \nabla \cdot \mathbf{u})\, \mathbf{1} + \Pi_2 + \Pi_3,$$

$$\mathbf{S} \;=\; \tfrac{1}{2}\left(\mathbf{L}+\mathbf{L}^T\right) - \tfrac{1}{3}\left(\nabla\cdot\mathbf{u}\right)\mathbf{1}, \quad \mathbf{L} \;=\; (\nabla\mathbf{u})^T$$

$$\tau_1 \;=\; 0.3211\left(\frac{\mu}{p}\right), \quad \tau_2 \;=\; 0.58775\left(\frac{\mu}{p}\right).$$

Here τ_1 and τ_2 are relaxation times, $\mathbf{L}$ is the velocity gradient, $\mathbf{S}$ the deviatoric part of the strain-rate tensor, μ the shear viscosity, ζ the bulk viscosity and $\mathbf{1}$ the identity tensor; Π_2 and Π_3 are higher order terms. In the limits of τ_1, $\tau_2 \to 0$ and Π_2, $\Pi_3 \to 0$, we recover the standard Newtonian model for the stress deviator:

$$\Pi \equiv \Pi^{eq} = -2\mu\mathbf{S} - \left(\zeta\nabla\cdot\mathbf{u}\right)\mathbf{1}.$$

Neglecting the higher-order terms, an expression for the first normal stress difference can be obtained for the steady uniform shear flow:

$$\mathcal{N}_1 = \left[\frac{6\gamma^2\tau_1}{3+\gamma(2\tau_1-\tau_2)(1+\gamma\tau_1+2\gamma\tau_2)}\right]\left(\frac{\mu}{p}\right), \tag{11}$$

where γ is the shear rate. This quantity is *positive* since the denominator remains positive (i.e. $2\tau_1 > \tau_2$ in the Boltzmann limit), as in our simulation results for dilute flows. Similarly, the expression for the second normal stress difference is

$$\mathcal{N}_2 = -\left[\frac{3\gamma^2(2\tau_1-\tau_2)}{3+\gamma(2\tau_1-\tau_2)(1+\gamma\tau_1+2\gamma\tau_2)}\right]\left(\frac{\mu}{p}\right). \tag{12}$$

This is *negative* as in our simulations for dilute flows.

As pointed out in our recent work (Alam & Luding 2003a), the above stress evolution equation (10) does not satisfy the *principle of material frame indifference* (MFI) which states that the constitutive laws should be *invariant* under rigid-rotation.

An interesting question is to look for the possibility of modelling normal stress differences using the standard frame-indifferent relaxation type models. In this regard, we had suggested an evolution equation:

$$\Pi + \tau_1\frac{\mathcal{D}\Pi}{\mathcal{D}t} = -2\mu\left(\mathbf{S} + \frac{\lambda}{2\mu}\left(\nabla\cdot\mathbf{u}\right)\mathbf{1} + \tau_2\frac{\mathcal{D}\mathbf{S}}{\mathcal{D}t}\right) \tag{13}$$

with $\mathcal{D}/\mathcal{D}t$ being the Jaumann derivative (Bird 1979). Here the two relaxation times, $\tau_1 = \tau_1(\nu, e)$ and $\tau_2 = \tau_2(\nu, e)$, are, in general, functions of both density and restitution coefficient. This is similar to the two-parameter Jeffrey's model, but the relaxation times should be interpreted carefully. It can be verified that the expressions for the first and second normal stress differences can be positive/negative depending on the values of τ_1 and τ_2. Thus, the frame-indifferent relaxation models can be used to predict positive and negative normal stress differences.

5 CONCLUSION

Granular fluids support large *normal stress differences* for the whole range of densities, clearly indicating their non-Newtonian rheology. One of the most important features of both rapid and quasi-static granular flows is anisotropy. Any anisotropic deformation will typically lead to anisotropic stress response but also to anisotropic change of structure or collision angle distribution. Normal stress differences are related to anisotropy, however, a vanishing normal stress difference does not imply vanishing anisotroy, it rather corresponds to anisotropy oriented in $\phi_A = \pi/4$ direction in the corresponding plane. A sign reversal corresponds to the rotation of the anisotropy from $\phi_A > \pi/4$ to $\phi_A < \pi/4$, or vice-versa.

We showed that both the *first* ($\mathcal{N}_1$) and *second* ($\mathcal{N}_2$) normal stress differences undergo *sign-reversals* with density. While the first normal stress difference changes its sign in the *dense* limit, the second normal stress difference changes its sign in the *dilute* limit. The *origin* of the *sign-reversal* of $\mathcal{N}_1$ is tied to a preferred value of the average collision angle, $\theta_{av} = \pi/4 \pm \pi/2$, averaged over the *upstream*-faces of the colliding particles. We have outlined a frame-indifferent constitutive model for granular fluids which allows the *sign-reversals* of both first and second normal stress differences, and thus allows for constituve modeling of arbitrary anisotropy.

REFERENCES

Alam, M. & Luding, S. 2003. Rheology of bidisperse granular mixtures via event-driven simulations. *J. Fluid Mech.* 476: 69.

Alam, M. & Luding, S. 2003a. First normal stress difference and crystalization in a dense sheared granular fluid. *Phys. Fluids.* 15(8): 2298-2312.

Allen, M.P. & Tildesley, D.J. 1989. *Computer Simulations of Liquids*. Clarendon Press, Oxford.

Bird, R.B., Armstrong, R.C. & Hassager, O. 1977. *Dynamics of Polymeric Liquids*. John Wiley Sons, London.

Campbell, C.S. 1989. The stress tensor for simple shear flows of a granular material. *J. Fluid Mech.* 203: 449-473.

Goldhirsch, I. 2003. Rapid granular flows. *Ann. Rev. Fluid Mech.* 35: 267-293.

Jenkins, J.T. & Richman, M.W. 1988. Plane simple shear of smooth inelastic circular disks: the anisotropy of the second moment in the dilute and dense limit. *J. Fluid Mech.* 192: 313-331.

Jin, S. & Slemrod, M. 2001. Regularization of the Burnett equations for rapid granular flows via relaxation. *Physica D.* 150: 207.

Sela, N. & Goldhirsch, I. 1998 Hydrodynamic equations for rapid flows of smooth inelastic spheres to Burnett order. *J. Fluid Mech.* 361: 41-75.

Zhang, D.Z. & Rauenzahn, R.M. 1997. A viscoelastic model for dense granular flows. *J. Rheol.* 41: 1275.